ELSEVIER

Thermochimica Acta 276 (1996) 161–174

thermochimica acta

# The Perkin–Elmer 1020 series thermal analysis system

C.Y. Zahra, A.-M. Zahra *

*Centre de Thermodynamique et de Microcalorimétrie, C.N.R.S. 26, rue du 141ème R.I.A., F-13331 Marseille Cedex 3, France*

Received 14 April 1995; accepted 20 September 1995

**Abstract**

The performance of a Perkin–Elmer 1020 Series DSC7 Thermal Analyser has been tested between 20 and 700°C with respect to isothermal and dynamic baseline stabilities, sample and instrumental time constants, thermal resistances, and measurement of temperatures, heats and heat capacities. The system includes software which meets the demands of industry, but is unsatisfactory for research. The arrangement of the thermoelectric coolers enables thermal equilibrium to be achieved in a short time, minimizes the isothermal drift, and makes it possible to start programming from subambient temperatures.

*Keywords:* Calibration; DSC; Thermoelectric coolers

## 1. Introduction

Before describing the performance of a DSC apparatus belonging to the 1020 series thermal analysis system manufactured by Perkin–Elmer in 1991 and based on the power-compensation principle, some generalities are reviewed, thereby introducing important parameters.

In the calorimeter head, the sample and reference cells are mounted symmetrically and heated by separate Pt furnaces; their temperatures are measured using Pt thermometers. Two electrical control loops operate on a time-sharing basis [1]. An average temperature loop compares the average temperature of the cells to that of the programmer and adjusts the power supply to the furnaces. The differential temperature loop which lags the power input controls the temperature difference between the cells and determines the differential power required to compensate for any temperature

* Corresponding author.

Elsevier Science B.V.
*SSDI* 0040-6031(95)02752-1

difference, via a proportional regulation. As there is no total compensation, small temperature differences persist and cause asymmetrical heat leaks by radiation and convection [2].

The dynamic baseline would correspond to the temperature axis if reference and sample cells as well as their thermal links to the calorimeter bath held at constant temperature were rigorously identical, which is never the case. Its deviation from a horizontal line may be minimized by applying an extra current to one of the cells. This results in temperature differences between sample and reference which may attain several degrees [3] and increase the asymmetrical heat leaks.

The thermal resistance $R_0$ between thermometer and sample is composed of two parts: a fixed resistance determined by the path between the thermometer and the cell bottom, and a contribution corresponding to the thermal resistances between cell bottom and sample via the sample pan. This contribution varies with the experimental set-up and should be as small as possible so that $R_0$ remains approximately constant.

The temperature difference $\Delta T$ between sample and thermometer is conveniently determined from fusion experiments, as the temperature of the sample remains constant during this phase transition. The thermal lag is given by [4]

$$\Delta T = T_{\mathrm{fus}(\beta)} - T_{\mathrm{fus}} = \Delta T_c + \beta\tau \tag{1}$$

with $T_{\mathrm{fus}}$ being the actual melting temperature in K (or $\theta_{\mathrm{fus}}$ in °C), $T_{\mathrm{fus}(\beta)}$ the observed onset temperature of melting at the heating rate $\beta$; $\tau$ is a time constant and $\Delta T_c$ a temperature scale offset independent of $\beta$, but dependent on all parameters which influence the asymmetrical heat leaks.

From fusion experiments, two other important parameters may be deduced. According to Gray [5], the slope characterizing steady state fusion is equal to $1/R_0$. The decay after the end of fusion obeys the law $\exp(-t/\tau_s)$, $\tau_s$ being the time constant of the sample. It is assumed [4] that $\tau_s$ is equal to $R_0C_s$, $C_s$ being the sum of the heat capacities of sample and pan. It is furthermore admitted that the overall time constant $\tau$ includes that due to the electrical circuitry of the DSC instrument, $\tau_{\mathrm{DSC}}$, in an additive manner, according to

$$\tau = \tau_{\mathrm{DSC}} + \tau_s = \tau_{\mathrm{DSC}} + R_0C_s \tag{2}$$

It follows that the thermal lag depends on the mass, shape and nature of the sample and sample pan, implying that calibration substances must have geometries, heat capacities and thermal conductivities similar to those of the samples to be investigated. $\Delta T$ varies also with the nature of the inert gas and its flow rate, and with the temperatures of the calorimeter bath, head and pivoting lid.

In the following, the characteristics of an instrument belonging to the 1020 Series DSC-7 Thermal Analysis System manufactured by Perkin–Elmer are determined and compared to those of the models DSC-2, -4 and -7. They all are equipped with the same calorimeter head (reference 0319 0006 or 0007 if tested at subambient temperatures). The manufacturer provides a 9-pin printer and a simple computer PC XT 8088 with software for easy use in industrial laboratories, without disclosing the procedures chosen; no facilities for self-programming are given. The system is delivered with the following specifications: calorimetric sensitivity, 10 μW; calorimetric uncertainty, less

than ±0.1%; calorimetric inaccuracy, less than ±1%; temperature uncertainty, ±0.1 K; temperature inaccuracy, ±0.1 K.

## 2. Baseline stability

The quality of the *dynamic baseline* recorded with empty cells depends on the symmetry achieved between reference and sample sides during the assembling of the calorimeter head. Because of the programming from subambient temperatures, the present apparatus possesses a head that has already been tested at very low temperatures.

In order to optimize the baseline, its slope and curvature are adjusted with the help of two simple potentiometers. The settings which assure least variation must not deviate strongly from the perfect symmetry position and are maintained constant: a change in the curvature setting leads to a change in the calibration values. The asymmetry between reference and sample sides may be estimated by melting a substance alternately on the reference and the sample side. With the chosen control dial settings, the onset temperatures of melting differ by about 1.3 K when heating a small bead of In in an Al pan at a rate of 20 K $min^{-1}$.

A constant heat sink temperature is provided by circulating water in the chamber beneath the calorimeter block. The apparatus is kept at (20±0.2)°C by air conditioning and starts to be controlled at about 20°C above the bath temperature (see the steps in Fig. 1). Argon is used at a flow rate of 16.5 ml $min^{-1}$ (inlet gas pressure $10^5$ Pa). A strong evolution of the baseline can be observed when the head is quite new, followed by a slower one over months, and years, as may be anticipated from experience gained on a DSC-4 model. This instability constitutes a serious inconvenience for a series of experiments that lasts more than one day.

The best baseline selected in November 1993 and shown in Fig. 1 differs from a straight line by about 0.5 mW between 40 and 600°C, and by about 1 mW between 40 and 700°C. In the case of a DSC-4 instrument equipped with a 0006 head, deviations of less than 0.5 mW are observed up to 600°C. In both cases, the repeatability of the baseline is very bad, and there is no systematic trend in its evolution over more than one year (see Fig. 1 which does not take account of the first month of use). Whereas the quality of the head purchased seems to be a matter of chance, the quality of the electronics used in the 1020 system is excellent: the programming is perfect, even at very low rates, and no longer produces steps in the records. Scan rates of 0.1–200 K $min^{-1}$ are available in steps of 0.1 K; the numerical values are correct.

The digit represents 1/10 000 of the full scale *Y*-range chosen, except for the ranges below 10 mW; the highest value still measured corresponds to ±3.2 times the full scale. Choosing the 10 mW range, for example, the digit takes a value of 1 μW and heat effects between ±32 mW can be measured. The heat flux noise is of some μW during heating up to high temperatures.

The short-time noise of the *isothermal baseline* was assessed with the calorimeter head either being empty or containing one sapphire disk. In the latter case, the fluctuations are about two times stronger than those characterizing the equilibrated

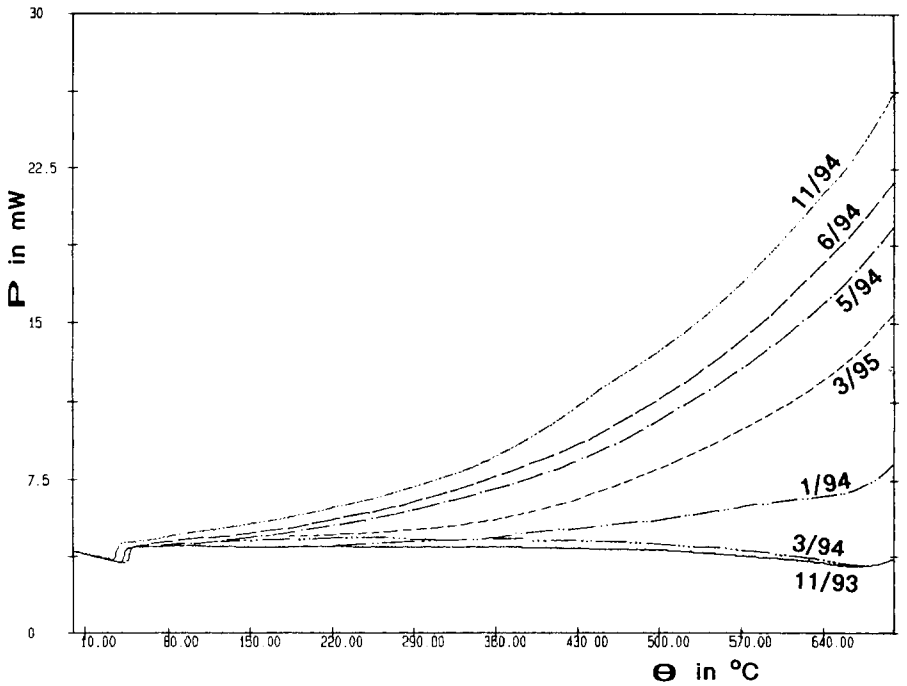


Fig. 1. Baseline of empty DSC apparatus taken at different periods (month/year) at a heating rate of 20 K min$^{-1}$.

condition for which the following values are found at a full-scale range of 2 mW: $\pm 2.5$ μW at 100°C, $\pm 5$ μW at 200°C, $\pm 25$ μW at 400°C, $\pm 20$ μW at 600°C. Hence signals falling below these levels cannot be detected.

A slow baseline drift was observed at constant temperatures and attributed to a slight variation of the water temperature in the closed loop due to heating of the cells and heat given off by the water circulating pump (4 W). It takes 10 h to reach a stationary state. Patt et al. [10] attained temperature constancy after 5 h when cooling the bottom of the aluminium block by partial immersion in an ice bath.

In order to improve the isothermal baseline behaviour and to start programming from lower temperatures without using ice or a cryostat, we have designed a new type of heat sink at constant temperature which involves 4 thermoelectric coolers utilizing the Peltier effect (Melcor $30 \times 30 \times 3.2$ mm$^3$; 33.4 W) and assures a temperature constancy of better than 10 mK. They are fixed between the calorimeter block and the water-cooled chamber which evacuates the heat transferred by the thermobatteries. For more details, see Ref. [7]. Thermal equilibrium is established within 15–60 min.

At 50°C, a heat flux noise of $\pm 1$ μW is observed; this determines the highest sensitivity of the apparatus. The drift falls below 1 nW s$^{-1}$ after 1 h. Although the manual foresees experimental times up to 2000 min, difficulties in the software arise when exceeding 4 h. At 400 (600)°C, noise and drift are $\pm 25$ ($\pm 20$) μW and $< 3$ ($< 6$) nW s$^{-1}$, respectively. Hence the noise level is not affected by the modifications. Fig. 2

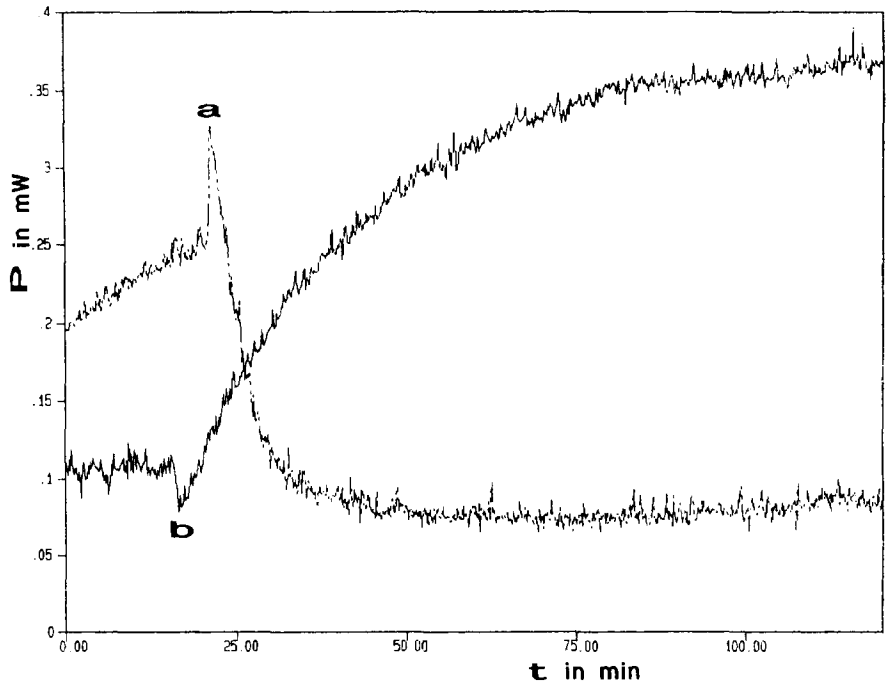


Fig. 2. Baseline evolution at 600°C when connecting thermoelectric modules (a) and when disconnecting them (b).

shows the baseline response when switching on (a) or off (b) the Peltier current, the calorimeter head being at 600°C and the cold junctions of the thermoelectric modules at 18°C.

In any experiment, the position of the electrical zero is unknown, which excludes correct appreciation of the baseline evolution and certain applications (see Ref. [8]).

## 3. Temperature calibration and time constants

The software of the 1020 system imposes temperature calibration in the scanning mode according to the two-point method based on the melting temperatures of calibration substances; intermediate temperatures are obtained by linear interpolation. The procedure is extremely simple, as it is only necessary to feed into the computer two pairs of values, the actual and the observed transition temperatures of two reference materials which limit the temperature range of interest. Recent recommendations [9] confirm that In, Sn, Pb and Zn may be used without any problems in conjunction with oxidized Al pans or with $Al_2O_3$ crucibles. Perkin–Elmer supplies In and Zn samples in crimped Al pans.

In order to study the dependence of the measured fusion temperature (as well as of the measured fusion enthalpy) on the experimental conditions, different sample and

pan assemblies were heated at various rates. Flat contact surfaces must be assured whenever possible. The onset melting temperatures, $T_{fus(\beta)}$ or $\theta_{fus(\beta)}$, are read at the intersection of the slope characterizing steady state fusion, with the linearly extrapolated initial baseline. According to Eq. (1), the time constant is then obtained by plotting the observed melting temperatures against heating rate. By extrapolating to $\beta = 0$, $T_{fus(o)}$ is derived. It deviates from the literature value for $T_{fus}$ by $\Delta T_c$ which may assume positive or negative values.

The variation of $\theta_{fus}$ with $\beta$ is shown in Fig. 3 up to a heating rate of 100 K min$^{-1}$ for the Zn sample supplied by Perkin–Elmer. In behaves similarly, i.e. the variation is approximately linear up to 20 K min$^{-1}$ (Fig. 4). Table 1 summarizes, for the three metals studied, the experimental set-up as well as the values for $\theta_{fus(o)}$, $\tau$, $\tau_s$, $R_o^{(1)} = \tau_s/C_s$ and $R_o^{(2)}$ obtained from the slope of steady state fusion at 20 K min$^{-1}$. Only a few runs were carried out on Zn samples, as they rapidly changed their colour and thermal coupling was bad. Pb is easy to use, but is not yet accepted as a temperature standard.

Several remarks may be formulated. The observed melting temperatures and time constants depend strongly on the experimental conditions, confirming that calibration has to imitate as closely as possible the actual runs. In view of a study on 1 mm thick Al alloys, for example, calibration using 1 mm thick Al samples with a small hole on the upper face which receives a small bead of a fusion calibration substance is recommended, in order to assure similar $R_o$ and $C_s$ values. By far the lowest time constant is obtained when pressing a small quantity of Pb on an Al foil ($\tau = 5.6$ s). There is no

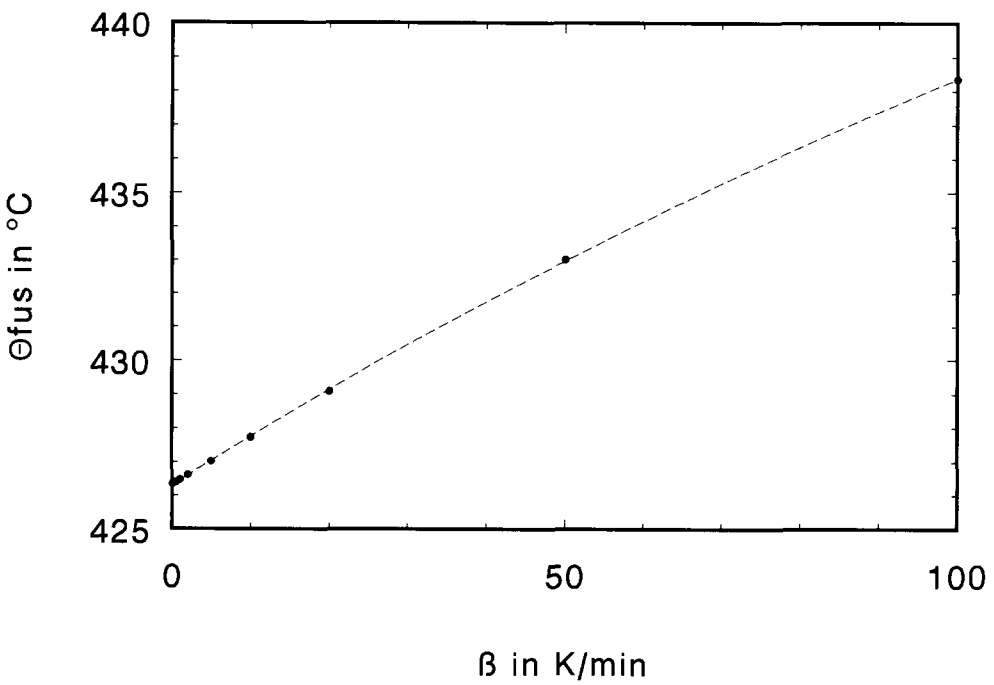


Fig. 3. Fusion temperature of Zn in crimped Al pan, in dependence of scanning rate.

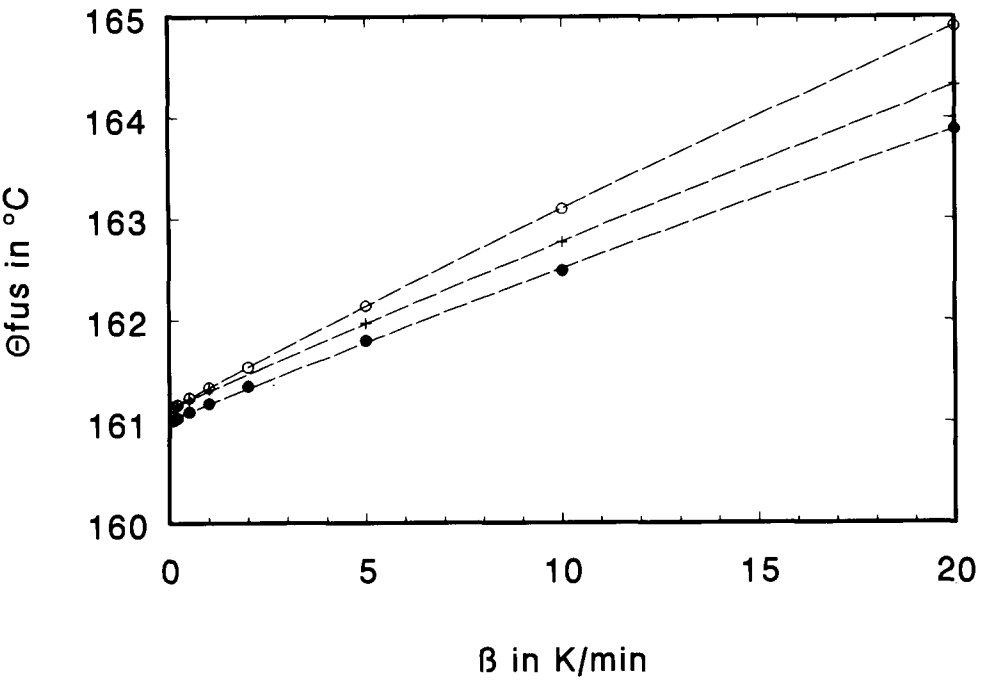


Fig. 4. Melting temperature of In as a function of heating rate: ●, In in crimped Al pan; +, on 1 mm thick Al; ○, on 1 mm thick $Al_2O_3$.

Table 1
Dependence of characteristic values on experimental set-up

| Metal | Symbol | $\theta_{fus(o)}$/°C | $\tau$/s | $\tau_s$/s | $R_o^{(1)}$/K mW$^{-1}$ | $R_o^{(2)}$/K mW$^{-1}$ |
|---|---|---|---|---|---|---|
| Indium | | | | | | |
| 6.7 mg in crimped Al pan | ◆ | 161.04 | 8.62 | < 1 | < 0.038 | 0.033 |
| 5.4 mg on 1 mm thick Al | ○ | 161.14 | 9.62 | 2.0 | 0.029 | 0.044 |
| 5.4 mg on 1 mm thick $Al_2O_3$ | Δ | 161.15 | 11.37 | 2.8 | 0.026 | 0.152 |
| Lead | | | | | | |
| 1.9 mg on 0.05 mm thick Al, flattened | ● | 333.66 | 5.62 | | | |
| 7.6 mg on 0.05 mm thick Al | ● | 334.11 | 7.21 | | | |
| 7.6 mg on 0.1 mm thick $Al_2O_3$ | ∇ | 334.02 | 8.65 | | | 0.35 |
| 100.0 mg in crimped Al pan | ◆ | 334.08 | 8.71 | 1.5 | 0.036 | 0.035 |
| 17.9 mg in crimped Al pan | ◆ | 334.04 | 8.82 | 1.3 | 0.043 | 0.050 |
| 4.7 mg in crimped Al pan with 2 covers | ◆ | 334.23 | 9.38 | 1.8 | 0.048 | 0.089 |
| 7.6 mg in Al pan on 0.1 mm thick $Al_2O_3$ | ∇ | 334.44 | 9.78 | 1.2 | 0.027 | 0.31 |
| 7.6 mg in Pt pan on 0.1 mm thick $Al_2O_3$ | ∇ | 334.50 | 10.29 | 1.6 | 0.025 | 0.32 |
| 7.6 mg on 1 mm thick Al | ○ | 335.25 | 10.86 | 1.6 | 0.021 | 0.80 |
| 7.6 mg on 1 mm thick $Al_2O_3$ | Δ | 334.26 | 12.09 | 2.8 | 0.023 | 0.32 |
| Zinc | | | | | | |
| 2.6 mg in crimped Al pan | ◆ | 426.34 | 8.23 | 0.9 | 0.030 | 0.056 |

systematic trend between $\theta_{fus(o)}$ and $\tau$ or $R_o$; in fact, its deviation from $\theta_{fus}$ is determined by asymmetrical heat leaks.

Following Eq. (2), the time constants are plotted in Fig. 5 as a function of the sum of the heat capacities; the scatter is important. If a straight line is traced through all the points, a mean value for $R_o$ of 0.044 K mW$^{-1}$ is obtained and $\tau_{DSC}$ is equal to 7.1 s. The former value compares well with $R_o^{(1)}$ of Table 1, and the latter with the difference between $\tau$ and $\tau_s$ for crimped Al pans. If only the three extreme $C_s$ values are taken into consideration, $R_o$ is 0.054 K mW$^{-1}$ and $\tau_{DSC}$ becomes equal to 5.5 s. The latter is still rather high and implies that the 1020 system incorporates substantial filtering. For comparison, the DSC-2 and -4 models are characterized by instrumental time constants of about 2.5 s [6,10], and the DSC-7 model by 4 s [11].

The mean values for $R_o$ obtained from Fig. 5 may be compared with the individual ones derived from each melting endotherm either directly from its initial slope ($R_o^{(2)}$) or its exponential decay ($R_o^{(1)}$). Table 1 shows that all $R_o^{(1)}$ values are not very different from the mean $R_o$, whereas $R_o^{(2)}$ becomes important as expected when using 0.1 mm thick $Al_2O_3$ or 1 mm thick Al supports.

Specimens encapsulated in standard Al pans with the help of the Perkin-Elmer crimper press show very good agreement between the different $R_o$ values, and their use is recommended whenever possible. Their $\tau$ and $\tau_s$ variations with temperature are not significative (Table 1). Smaller $\tau$ values of (5.4 ± 1.8) s have been assessed for a great number of metallic as well as organic substances encapsulated in Al pans and examined

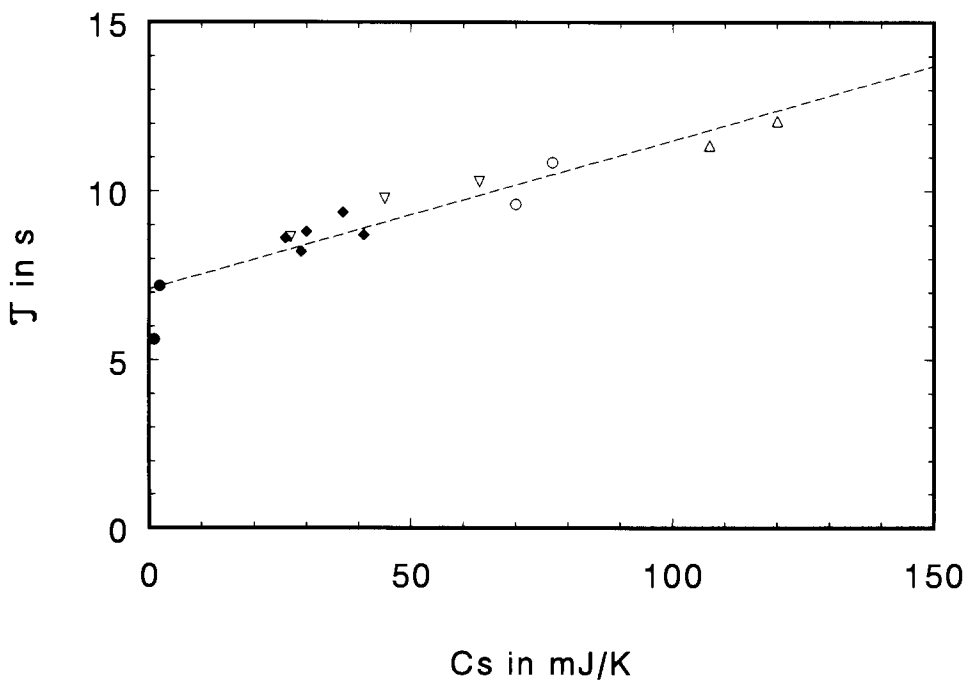


Fig. 5. Relation between time constants and heat capacity values (see Table 1 for symbols).

with the help of a DSC-7 [12]. $R_0$ values of about 0.07 K mW$^{-1}$ were published for all DSC models [6, 10, 11].

In the case of fusion experiments carried out at 20 K min$^{-1}$ on the In and Zn samples supplied by Perkin–Elmer, a repeatability of $\pm 0.03$ K is observed when $\theta_{fus(o)}$ is determined ten times without external intervention. If the samples are taken off completely and remounted after each run, the repeatability is $\pm 0.10$ K for In and $\pm 0.15$ K for Zn. Höhne and Glöggler [2] observed a repeatability of $\pm 0.02$ K, probably without touching the specimens between the runs.

The temperature scale of the 1020 system was calibrated at 20 K min$^{-1}$ by noting the fusion temperatures of In and Zn supplied by Perkin–Elmer. The mean temperatures for ten runs were entered into the software program together with the melting temperatures of In and Zn according to the International Temperature Scale of 1990 [13]. Then the calibration was checked by repeating the experimental series on In and Zn and by examining Sn, Cd and Pb samples of purity $\geq 99.99\%$, all encapsulated in Al pans. The melting temperatures of the last two metals are not accepted as fixed points, but are taken from Ref. [14]. In Table 2, the literature values for $\theta_{fus}$ and the observed deviations therefrom are listed. The accuracy achieved is not quite as good as that claimed by Perkin–Elmer. According to Ref. [10], an inaccuracy of $\pm 0.1$ K is only obtainable under rigorous experimental conditions including small sample size (2–20 mg in general), low heating rate, and constant gas flow rate, bath temperature and level.

In isothermal temperature calibration, the temperature is increased by 0.1 increments and that corresponding to fusion of a pure substance is noted (see Ref. [3]). This method has the advantage of being free from thermal lag, but cannot be carried out in a simple manner with the 1020 system.

## 4. Heat flux and heat calibration

The most recent recommendations for calibration of scanning calorimeters are given in Ref. [15]. As a consequence of the small temperature differences between sample and reference cells, calibration factors depend on temperature, heating rate, heat flow and sample parameters. Although their variation is much less than in the case of heat flux DSC, it must be taken into account for precise work.

A power-compensated DSC apparatus measures directly the heat flux $P$ absorbed or liberated by the sample. These readings may be calibrated by $c_p$ measurements. Heat

Table 2
Deviations of temperatures and heats of fusion from literature values

| Metal | Mass/mg | $\theta_{fus}$/°C | $\Delta\theta$/°C | $\Delta H_{ref}$/J g$^{-1}$ | $\Delta H_{meas} - \Delta H_{ref}$/% |
|---|---|---|---|---|---|
| In | 4.7983 | 156.5985 | 0.22 | (28.71 ± 0.08) [17] | +0.1 |
| Sn | 10.8089 | 231.928 | 0.07 | (60.47 ± 0.13) [17] | +0.95 |
| Zn | 3.0497 | 419.527 | 0.14 | (107.45 ± 0.61) [18] | +0.05 |
| Cd | 9.6561 | 321.07 | 0.27 | 55.09 [13] | −0.3 |
| Pb | 17.8770 | 327.46 | 0.01 | 23.04 [13] | +0.96 |

capacity standards provide values at any temperature which are transformed into heat flows by multiplication with the scan rate (more truly, with the heating rate of the sample).

The heat capacity indications of the 1020 system were checked at various temperatures with the help of a sapphire disk. The calibration factor $k_1 = c_{p,\mathrm{lit}}/c_{p,\mathrm{meas}} = c_{p,\mathrm{lit}}\beta/P_{\mathrm{meas}}$ varied by 5% between 100 and 700°C.

Enthalpy standards based on melting of pure substances lead to the determination of the calibration factor $k_2 = \Delta H_{\mathrm{fus,lit}}/\Delta H_{\mathrm{fus,meas}} = \Delta H_{\mathrm{fus,lit}}/\int_{\mathrm{meas}}^{\mathrm{p}} \mathrm{d}t$ at some specific temperatures only. As fusion is accompanied by very strong endothermal heat effects inducing differential heat leaks, these two calibration methods agree only within several %. Hence calibration must be carried out by fusion, if enthalpy values for transition are to be determined, and by $c_p$ measurements in the case of heat capacity studies.

Before the integration of heat effects, a baseline must be chosen. This task is the more difficult the greater the heat capacity change of the sample during the transition, as the displacement is proportional to $\Delta c_p \beta$ [5]. Several interpolated baseline constructions have been proposed which are summarized in Ref. [16]. According to these authors, their influence lies within the repeatability of the DSC method which they evaluate to $\pm 0.5\%$.

In order to avoid problems arising from unknown baselines, Flynn [3] proposes starting and finishing at constant temperatures $T_1$ and $T_2$ and connecting the steady state isothermal baselines linearly. This method has the advantage of showing the temperature variation of the enthalpy and of yielding correctly the fraction $\alpha$ reacted. It is not generally applicable, as phase evolution may occur during the isothermal holds. In the latter case, the approximate fraction transformed is obtained by dividing the heat effect integrated up to the temperature $T$ in question by the total heat effect $\Delta H$, the transformation rate being $(\mathrm{d}\alpha/\mathrm{d}t)_{\mathrm{T}} = P_{\mathrm{T}}/\Delta H$.

The software of the 1020 system foresees heat calibration at one temperature only, using a pure substance the melting enthalpy of which is well known. To this end, the fusion process of In encapsulated in an Al pan was studied ten times at 20 K $\mathrm{min}^{-1}$ without opening the calorimeter. The mean value obtained was then fed into the computer together with the fusion enthalpy of In given in the literature ($\Delta H_{\mathrm{ref}}$). The validity of this simple calibration procedure was checked by measuring the heats of fusion of Sn, Zn, Cd and Pb, as well as In again, and by comparing $\Delta H_{\mathrm{meas}}$ with the literature values. For Zn, the value indicated in the most recent publication [18] was chosen, but it has to be noted that this is much lower than in preceding studies. The results given in Table 2 are inaccurate to $\pm 1\%$ only, as announced by the manufacturer; their standard deviations $\sigma_{\mathrm{meas}}$ are slightly in excess of those indicated by Perkin–Elmer. The error in sample mass is negligible when using a high precision microbalance ($\pm 0.1$ μg).

In addition, the heats of fusion of In and Zn were determined ten times at 20 K $\mathrm{min}^{-1}$ using crimped-shut samples supplied by Perkin–Elmer, either without touching the experimental set-up or replacing the samples after each run. In the first case, the repeatability is better than $\pm 0.1\%$, but attains in the second case $\pm 0.7\%$ for In and $\pm 0.3\%$ for Zn. This confirms that the slightest change in the position of the sample pan,

or the sample and lids relative to the calorimeter cell influences the measurement, as the contact resistances are changed. The calorimetric imprecision of less than $\pm 0.1\%$ given by Perkin–Elmer presumably corresponds to repetitions without external intervention.

Fig. 6 shows the influence of heating rate on the heat of fusion for Pb samples in conjunction with the pan assemblies described in Table 1. The calorimeter was not opened between the individual runs and was not yet calibrated. The $\Delta H$ values increase slightly with heating rate, but are approximately constant between 5 and 20 K $min^{-1}$ and display a repeatability of $\pm 0.8\%$. When using 100 mg Pb instead of 7.6 mg, the heat of fusion apparently increases by 1.6% at 20 K $min^{-1}$.

An electrical calibration of the apparatus, as possible with the DSC-4 model, is not available.

## 5. Heat capacity determination

Two methods may be used in order to assess unknown heat capacities, the dynamic or scanning method and the integration or enthalpy method (see Refs. [3] and [19]). The sequence of the necessary runs is the same. An empty sample pan is heated (or cooled) at a constant rate between two isothermal temperatures $T_1$ and $T_2$. Then

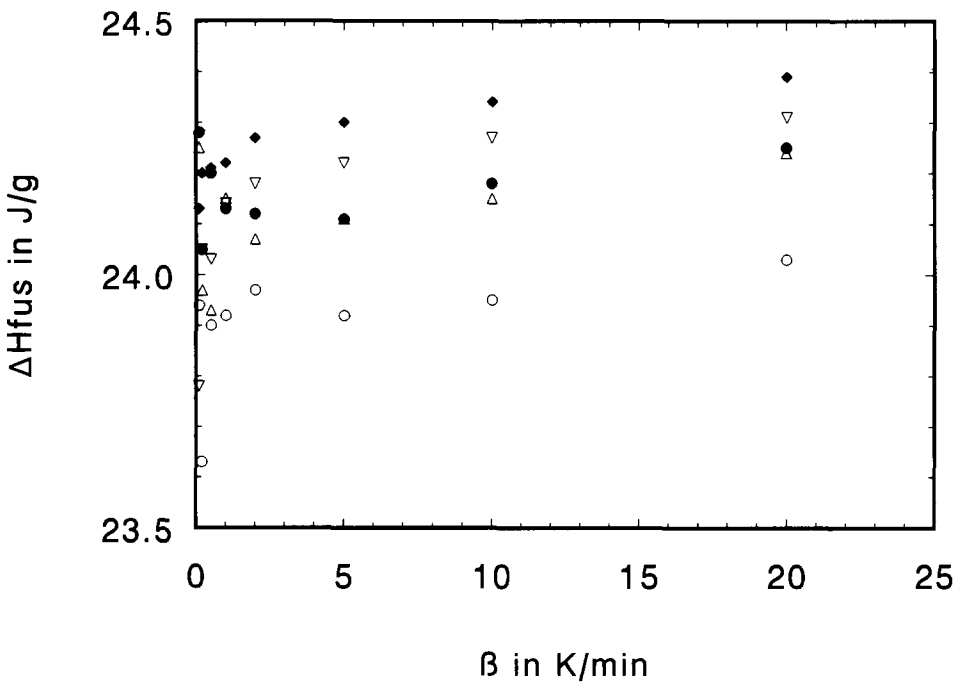


Fig. 6. Heat of fusion of Pb plotted against heating rate, for five different pan assemblies (see Table 1 for symbols).

a substance with well-known $c_{p,r}$ is heated within the pan and, finally, the specimen with the unknown heat capacity $c_{p,s}$. On the reference side, an empty pan is used during all three runs. Sapphire as calibrant has the advantage that its $c_p$ values (see Ref. [15]) cover the whole temperature range of a DSC apparatus.

In the dynamic method, the heat flows $P_r$ between the curves for empty pan and calibrant, and $P_s$ between empty pan and sample, both corrected for different isothermal baselines, are determined over a temperature interval of 20–100 K. Then $c_{p,s}$ is calculated from the equation

$$c_{p,s} = c_{p,r} m_r P_s / m_s P_r$$

The inaccuracy of the $c_p$ measurements is in general given as $\pm 1\%$. A repeatability of $\pm 0.5\%$ is stated by Ref. [2]. Difficulties arise from changing contact resistances and low thermal conductivities of the samples.

Problems associated with thermal lag are avoided by applying the enthalpy method and by integrating each curve with respect to its isothermal baseline recorded at $T_1$ and $T_2$ (normally 5–20 K apart). The area between the empty pan and the calibrant yields a calibration factor $k_3 = \Delta H_{lit}/\Delta H_{meas}$ which is not equal to $k_1$. The mean heat capacity of unknown samples is then derived from

$$c_{p,s} = k_3 \Delta H / m_s (T_2 - T_1)$$

$\Delta H$ being the enthalpy which corresponds to the area delimited by the specimen and the empty pan curves. For measurements of $c_p$ values which vary strongly with temperature, this method is to be preferred. Temperature calibration of the instrument has to be carried out in the isothermal mode (or at the smallest scan rate possible).

The software of the 1020 system allows automatic calibration of the apparatus by introducing the correction factor $k_1$ or $k_3$ which applies to the temperature interval under question. The values for $\Delta H$ are displayed, but it is not possible to perform a series of temperature steps automatically. The manual even proposes determining $c_p$ via $k_2$, which does not yield correct results; a 5% inaccuracy is observed when deriving $c_p$ values of sapphire via the fusion enthalpy of indium. For a rather ideal case, the $c_p$ determination of Al between 100 and 500°C [20], the inaccuracy is $\pm 0.5\%$ when using $k_1$. These studies were performed over a temperature interval of 20 K at a rate of 5 K $min^{-1}$.

## 6. Conclusions

The Perkin–Elmer 1020 Series DSC7 Thermal Analysis System is an entirely computer-controlled instrument with easy-to-handle software conceived for use by technicians in industrial laboratories. Its application to precise research work suffers from several shortcomings: It is not disclosed how the programs are written and their number is limited. Indication of the interface which would allow self-programming is not given. Several claims in the manual are not correct. The baseline instability seems to be a feature of all power-compensated DSC instruments and limits measurements in time. The time constant is higher than in the case of the other DSC models, introducing

more substantial curve distortions. The electrical zero of the instrument is floating, which excludes interesting applications.

Positive points are the performances which, for simple reactions, are not far off the specifications given by Perkin–Elmer.

When studying fusion processes of pure metals, the standard deviation of mean heats is less than $\pm 0.2\%$ in the absence of external intervention. The accuracy achieved depends on the accuracy with which the melting enthalpies of convenient reference substances are known. If one admits that the most recent value for zinc is correct, an accuracy of 99% is obtained with the calibration program of Perkin–Elmer. But doubts exist as long as the heats of fusion of Zn, Cd and Pb are not reassessed by precise calorimetric methods.

Temperature differences due to thermal lag depend on sample- and instrument-dependent parameters. The Perkin–Elmer model allows automatic correction of these lags, provided utmost care has been taken to duplicate the measuring conditions during the calibration runs. A temperature inaccuracy of about 0.2 K is observed with respect to three fixed points on the International Temperature Scale. The standard deviation of the mean value is less than $\pm 0.1$ K, if the calorimeter head is not opened between the runs. The experimental results are thus of high quality, but of limited exploitation due to the imposed software.

The arrangement of the thermoelectric coolers makes it possible to start programming from lower temperatures and assures an excellent constancy of the calorimeter bath temperature, which is, moreover, achieved more rapidly than by conventional methods.

## Acknowledgement

The authors are indebted to G. de Bardon de Segonzac who proposed and realized the use of thermoelectric coolers.

## References

[1] E.S. Watson, M.J. O'Neill, J. Justin and N. Brenner, Anal. Chem., 36 (1964) 1233.
[2] G.W.H. Höhne and E. Glöggler, Thermochim. Acta, 151 (1989) 295.
[3] J.H. Flynn, Thermochim. Acta, 217 (1993) 129.
[4] J.H. Flynn, in R.S. Porter and J.F. Johnson (Eds.), Analytical Calorimetry, Vol. 3, Plenum Press, New York, 1974, p. 17.
[5] A.P. Gray, in R.S. Porter and J.F. Johnson (Eds.), Analytical Calorimetry, Vol. 1, Plenum Press, New York, 1968, p. 209.
[6] E.J. Cotts, in R.D. Shull and A. Joshi (Eds.), Thermal Analysis in Metallurgy, The Minerals, Metals & Materials Society, 1992, p. 299.
[7] C.Y. Zahra, G. de Bardon de Segonzac and A.-M. Zahra, Journèes de Cal. Anal. Therm., 26 (1995) 363.
[8] S.M. Sarge, Thermochim. Acta, 187 (1991) 323.
[9] H.K. Cammenga, W. Eysel, E. Gmelin, W. Hemminger, G.W.H. Höhne and S.M. Sarge, Thermochim. Acta, 219 (1993) 333.

[10] M.E. Patt, B.E. White, B. Stein and E.J. Cotts, Thermochim. Acta, 197 (1992) 413.
[11] G.L. Batch and C.W. Macosko, Thermochim. Acta, 188 (1991) 1.
[12] G.W.H. Höhne, H.K. Cammenga, W. Eysel, E. Gmelin and W. Hemminger, Thermochim. Acta, 160 (1990) 1.
[13] H. Preston-Thomas, Metrologia, 27 (1990) 3.
[14] A.T. Dinsdale, Calphad, 15 (1991) 317.
[15] S.M. Sarge, E. Gmelin, G.W.H. Höhne, H.K. Cammenga, W. Hemminger and W. Eysel, Thermochim. Acta, 247 (1994) 129.
[16] W.F. Hemminger and S.M. Sarge, J. Therm. Anal., 37 (1991) 1455.
[17] F. Gronvold, J. Chem. Thermodyn., 25 (1993) 1133.
[18] D.A. Ditmars, J. Chem. Thermodyn., 22 (1990) 639.
[19] S.C. Mraw, in C.Y. Ho and A. Cezairliyan (Eds.), Specific Heat of Solids, Vol. 1–2, Cindas Data Series on Material Properties, Hemisphere Publ. Corp., New York, 1988, p. 395.
[20] P.D. Desai, Int. J. Thermophys., 8 (1987) 621.